

SANDIA REPORT

Unlimited Release
September 14, 2015

Predicting the Occurrence of Mixed Mode Failure Associated With Hydraulic Fracturing, Part 2 Water Saturated Tests

Stephen J. Bauer, Scott T. Broome, Charles Choens, and Perry C. Barrow

Prepared by
Sandia National Laboratories
Albuquerque, New Mexico 87185 and Livermore, California 94550

Sandia is a multiprogram laboratory operated by Sandia Corporation,
a Lockheed Martin Company, for the United States Department of Energy's
National Nuclear Security Administration under Contract DE-AC04-94AL85000.

Approved for public release; further dissemination unlimited.



Issued by Sandia National Laboratories, operated for the United States Department of Energy by Sandia Corporation.

NOTICE: This report was prepared as an account of work sponsored by an agency of the United States Government. Neither the United States Government, nor any agency thereof, nor any of their employees, nor any of their contractors, subcontractors, or their employees, make any warranty, express or implied, or assume any legal liability or responsibility for the accuracy, completeness, or usefulness of any information, apparatus, product, or process disclosed, or represent that its use would not infringe privately owned rights. Reference herein to any specific commercial product, process, or service by trade name, trademark, manufacturer, or otherwise, does not necessarily constitute or imply its endorsement, recommendation, or favoring by the United States Government, any agency thereof, or any of their contractors or subcontractors. The views and opinions expressed herein do not necessarily state or reflect those of the United States Government, any agency thereof, or any of their contractors.

Printed in the United States of America. This report has been reproduced directly from the best available copy.

Available to DOE and DOE contractors from

U.S. Department of Energy
Office of Scientific and Technical Information
P.O. Box 62
Oak Ridge, TN 37831

Telephone: (865) 576-8401
Facsimile: (865) 576-5728
E-Mail: reports@adonis.osti.gov
Online ordering: <http://www.osti.gov/bridge>

Available to the public from

U.S. Department of Commerce
National Technical Information Service
5285 Port Royal Rd.
Springfield, VA 22161

Telephone: (800) 553-6847
Facsimile: (703) 605-6900
E-Mail: orders@ntis.fedworld.gov
Online order: <http://www.ntis.gov/help/ordermethods.asp?loc=7-4-0#online>



Predicting the Occurrence of Mixed Mode Failure Associated With Hydraulic Fracturing, Part 2 Water Saturated Tests

Stephen J. Bauer, Scott T. Broome, Charles Choens, and Perry C. Barrow
Geomechanics Department
Sandia National Laboratories
P.O. Box 5800
Albuquerque, NM 87185-0735

Abstract

Seven water-saturated triaxial extension experiments were conducted on four sedimentary rocks. This experimental condition was hypothesized more representative of that existing for downhole hydrofracture and thus it may improve our understanding of the phenomena. In all tests the pore pressure was 10 MPa and confining pressure was adjusted to achieve tensile and transitional failure mode conditions. Using previous work in this LDRD for comparison, the law of effective stress is demonstrated in extension using this sample geometry. In three of the four lithologies, no apparent chemo-mechanical effect of water is apparent, and in the fourth lithology test results indicate some chemo-mechanical effect of water.

Acknowledgments

The authors would like to acknowledge Moo Lee and Erik Webb, Sandia National Laboratories, for their support of this work.

Table of Contents

ABSTRACT.....	3
ACKNOWLEDGEMENTS.....	4
LIST OF FIGURES.....	6
INTRODUCTION.....	7
EXPERIMENTAL METHODS.....	7
Sample Descriptions.....	7
Sample Preparation.....	8
Experimental Procedure.....	9
EXPERIMENTAL RESULTS.....	10
Image Comparison Results.....	14
DISCUSSION.....	18
ANTICIPATED IMPACT.....	18
CONCLUSIONS.....	19
REFERENCES.....	19

List of Figures

Figure 1. Sample geometry with layered jacketing system (after Choens, in prep).	9
Figure 2. Berea sandstone: Axial Strain vs Axial Stress wet and dry at 10 MPa effective confining pressure.....	11
Figure 3. Cararra Marble: Axial Strain vs Axial Stress wet and dry at 10 MPa effective confining pressure.....	11
Figure 4. Indiana Limestone: Axial Strain vs Axial Stress wet and dry at 20 MPa and 40 MPa effective confining pressure.....	12
Figure 5. Kansas Chalk: Axial Strain vs Axial Stress wet and dry at 10 MPa and 5 MPa effective confining pressure.....	13
Figure 6. Berea sandstone: Dry: top; Wet: bottom at 10 MPa effective confining pressure.....	14
Figure 7. Carrara Marble: Dry: top; Wet: bottom at 10 MPa effective confining pressure.....	15
Figure 8. Indiana Limestone: Dry: top; Wet: bottom at 20 MPa effective confining pressure....	15
Figure 9. Indiana Limestone: Dry: top; Wet: bottom at 40 MPa effective confining pressure....	16
Figure 10. Kansa Chalk: Dry: top; Wet: bottom at 5 MPa effective confining pressure.....	16
Figure 11. Kansa Chalk: Dry: top; Wet: bottom at 5 MPa effective confining pressure.....	17
Figure 12. Kansa Chalk: Dry: top; Wet: bottom at 10 MPa effective confining pressure.....	17

INTRODUCTION

The intent of this study is to extend the recent work of Choens (in prep) in terms of the understandings developed of the extension to shear transition in unconventional reservoir rocks; the nature of the extension is to complete some tests using the same experimental methods, however these tests are water saturated. This work is simply intended to conduct a limited number of water-saturated triaxial extension experiments; this condition may be more representative of that present in downhole hydrofracture conditions and therefore may improve our understanding of this phenomena. Hydraulic fracture is an important stimulation method in unconventional resources and enhanced geothermal. The experiments conducted take advantage of Sandia's unique high pressure geomechanics laboratory capabilities.

EXPERIMENTAL METHODS:

Sample Descriptions:

Four different rock types were used in this study, Berea Sandstone, Carrara Marble, Indiana Limestone, and Kansas Chalk.

The Berea sandstone samples were taken from a single block from the Cleveland Rock Quarry in Ohio. Previous studies on samples from this local have shown that the grain size, porosity, and mineralogy are comparable to other published measurements for Berea [Bobich, 2005; Menendez et al., 1996; Zhang et al., 1990]. In general, the samples consist of subangular, well-sorted grains composed of 75-80% quartz, 20-25% feldspar, and lesser amounts of dolomite, rutile, zircon, kaolinite, and some secondary minerals [Menendez et al., 1996; Zhang et al., 1990]. Dolomite grains and cement (up to 400 μ m) are distributed throughout the granular mass. Porosity measurements attained from mass differences between dry samples and samples saturated with alcohol or distilled waters range from 16-19%. The Schwawrtz-Saltykov method was used to determine the grain size distribution from measurements of grain diameter in plane petrographic sections; the mean diameter is 185 μ m [Hillard and Lawson, 2003; Zhang et al., 1990]. Bedding laminae, with spacing around 0.5 mm, are defined by concentration of mafic minerals visible on the hand sample scale. Previous studies on Berea have shown that the laminations influence fracture behavior [Herrin, 2008]. Samples were cored parallel to the laminations to minimize bedding effects on tensile fracture orientation.

Carrara marble samples were taken from a single block from the Lorano Bianco Carrara marble of Italy. This marble is nearly pure calcite and has less than 1% porosity. The calcite crystals are euhedral with triple point grain boundary intersections and they have a weak crystallographic preferred orientation. The grain sizes range from 250-355 μ m [Rodriguez, 2005]. The undeformed marble has occasional thin mechanical twins and sporadic, intragranular, cleavage microfractures that are a few microns in length [Fredrich et al., 1989; Pieri et al., 2001; Rodriguez, 2005].

Indiana limestone samples were taken from a single block of limestone. Indiana limestone is over 97% calcite with 15 to 20% porosity. It is a calcite-cemented grainstone, where the grains can be over 300 μm in diameter. Classified as a freestone for architectural purposes, the rock is homogeneous and contains no inherent parting planes in the material.

Kansas chalk samples were taken from a 20 inch diameter core purchased from TerraTek. The unit is a member of the Upper Cretaceous Niobrara Formation. This chalk is very pure, 99% calcite, with high porosity at 30%. Grain sizes are very small, 0.2 to 0.55 μm in diameter. Due to similarities in capillary behavior, Kansas chalk has long been used as an analog material for North Sea reservoir rocks. Additionally, the Niobrara Formation is now an active unconventional reservoir rock itself.

Sample Preparation:

The tests utilized a specialized sample geometry, the notch-cut, or ‘dogbone’ geometry. This particular sample geometry has been used in previous studies across the tensile to shear transition and has shown to produce consistent and reproducible results as compared to other sample geometries in the same stress field. To create the dogbone geometry, the samples are ground on a microlathe mounted on a stationary surface grinder to create the neck of the sample. Two inch diameter cores are mounted on the microlathe with the cylindrical axis perpendicular to the grinding wheel. The samples are ground down slightly, to 50.673mm inch diameter to ensure that the samples are perfectly round and the axis is true to the microlathe. To cut the neck, the microlathe is turned parallel to the grinding wheel. The diameter of the grinding wheel determines the radius of curvature of the neck, 88 mm. After the neck is finished, the sample is cut to length, and the ends are ground perpendicular to the axis. The final dimensions of the sample are 102 mm in length, 47 mm diameter at the shoulder, and 30 mm diameter at the neck. The geometry creates a stress concentration in the neck of the sample, allowing the deformation to be optimally located in this portion of the sample (Figure 1).

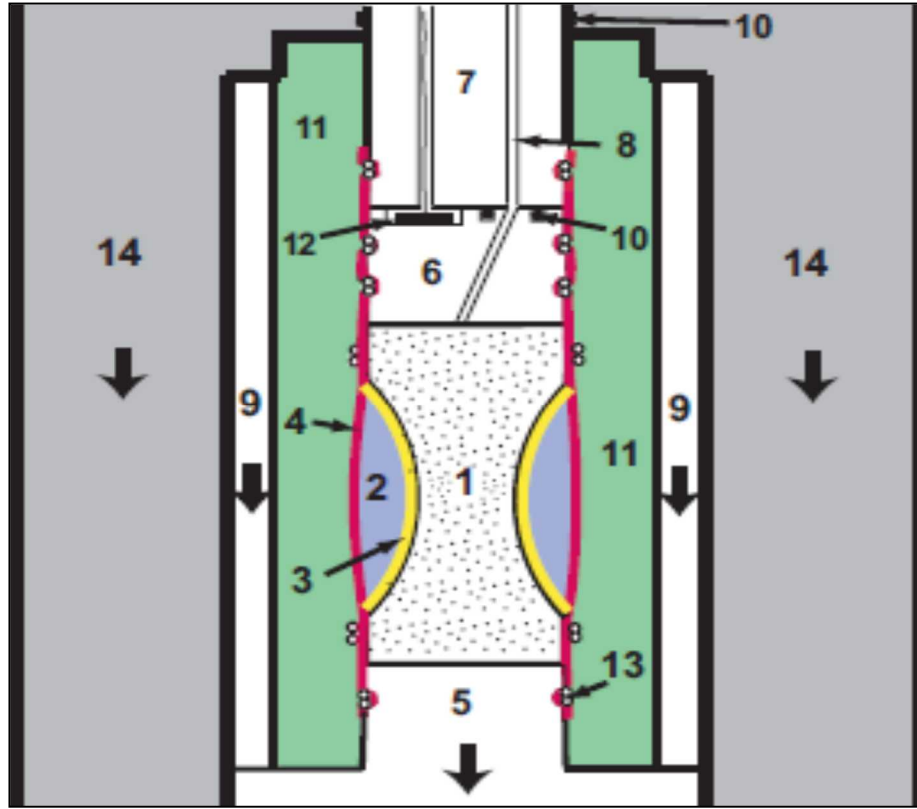


Figure 1. Sample geometry with layered jacketing system (after Choens, in prep). Important components include (1) rock sample, (2) placticene, (3) latex sheath, (4) polyolefin heat shrink jacketing, (5) lower piston, (6) upper closure, (7) upper piston, and (8) upper flow port [lower flow port not shown].

Maintaining jacket integrity pre and post failure while still transmitting the stresses from the confining medium necessitated a three layer jacketing procedure. The first layer was a 0.2 mm thick latex sheeting wrapped directly onto the sample. Previous studies have shown that the latex jacketing is extremely weak and does not affect the mechanical behavior of the sample while protecting the sample from the next layer, placticene modeling clay [Bobich, 2005; Ramsey and Chester, 2004]. The clay was used to fill the void in the sample created by the dogbone; the clay is extremely weak under pressure, transmitting the confining pressure to the neck of the sample while mechanically decoupling the jackets. The clay also prevents the edges from the shoulders from cutting the jackets. The assembly was isolated from the confining fluid by a layer of heat shrink polyolefin tubing sealed at the endcaps with nickel-chrome tie wires. The sample tie wires were coated with a layer of flexible UV cure epoxy for additional protection. Both ends of all samples were fitted with a pressed metal frit, to facilitate pore pressure access to both side of the sample.

Experimental Procedure

All experiments were conducted at Sandia National Laboratories at the Geomechanics Research Laboratory using a 1 MN load frame. The machine is capable of independent confining and pore pressure control, and contains electrical feedthroughs for sample instrumentation. Isopar, an

isoparaffinic fluid solvent, is the confining medium. Samples are deformed at an axial strain rate of 10⁻⁵ per second. Axial stress is measured with an external load cell; axial stress calculations consider pressure vessel piston friction in axial force determinations. Because of the arrangement of the sample assembly, the axial stress and confining pressure are independent. Samples are initially loaded to 1 MPa axial stress before confining pressure is added. The axial stress is increased at the same rate as the confining pressure, maintaining a 1 MPa differential stress on the sample. This small load ensures that the sample assembly remained in contact with the piston during the hydrostatic loading. Confining pressure is applied in ramped steps of ~3.5 MPa. At 3.5 MPa confining pressure, ~1 MPa pore pressure, was applied to the lower end of the sample until water came out the top pore pressure port. When this was observed, a second pore pressure pump was attached to the top pore pressure port. Depending on the lithology, this pressure saturation took up to a few hours. Confining pressure ramping continued to the test pressure, and pore pressure ramping continued as well, capping at 10 MPa (used for all tests). The pore pressure was then allowed to equilibrate one to two hours.

When the desired confining pressure is reached, the axial stress was decreased and the piston was reversed at a constant rate while the confining pressure is held constant; pore pressure was also held constant at 10 MPa using pumps on opposing sides of the sample. The confining pressure is the greatest principal stresses, σ_1 and σ_2 , and the axial stress is the least principal stress, σ_3 . Due to the difference in areas between the shoulders and necks of the samples, a tensile stress can be generated in the neck of the sample.

Seven triaxial extension experiments, all with 10 MPa pore pressure were conducted in this study. Test conditions were chosen first to compare strength at dry tensile pressure conditions, and secondly to compare strength at pressure conditions at or above the transition pressure from tension to shear.

Confining pressure of 20 MPa and pore pressure of 10 MPa (10 MPa effective confining pressure) is used for the Berea sandstone and Carrara marble tests. The two Indiana limestone samples are deformed at 50 and 30 MPa confining pressure, with 10 MPa pore pressure each, resulting in effective confining pressures of 40 MPa and 20 MPa, respectively. Kansas chalk samples are deformed at 20 and 15 MPa confining pressure, with 10 MPa pore pressure each, resulting effective confining pressures of 10 MPa and 5 MPa, respectively.

In this report we adopt the convention that compressive stress and contractive strains are positive. We will note the maximum and minimum principal stresses by σ_1 and σ_3 , respectively. The mean stress, $(\sigma_1 + \sigma_3) / 3$, is denoted by P , and the differential stress, $\sigma_1 - \sigma_3$, by Q . Axial strain was calculated using the actuator LVDT displacements, corrected for apparatus distortion.

RESULTS:

Results are presented in two forms, stress strain curves for each test, compared to the dry counterparts, and images of the samples compared to their dry counterparts.

The Berea Sandstone, at 10 MPa effective confining pressure, has a wet strength is ~12.5 MPa and the dry strength ~14.5 MPa, with strain at failure of 0.175% and 0.15%, respectively (Figure 2).

The Carrara Marble, at 10 MPa effective confining pressure, has a wet strength of ~21 MPa and the dry strength ~16 MPa, with strain at failure of 0.12% and 0.07%, respectively (Figure 3).

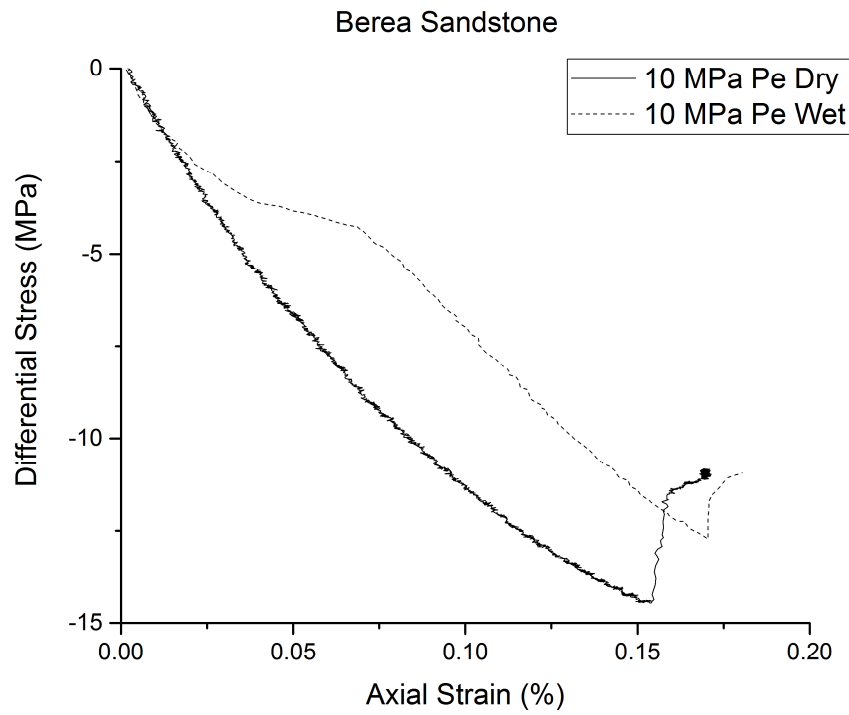


Figure 2. Berea sandstone: Axial Strain vs Axial Stress wet and dry at 10 MPa effective confining pressure.

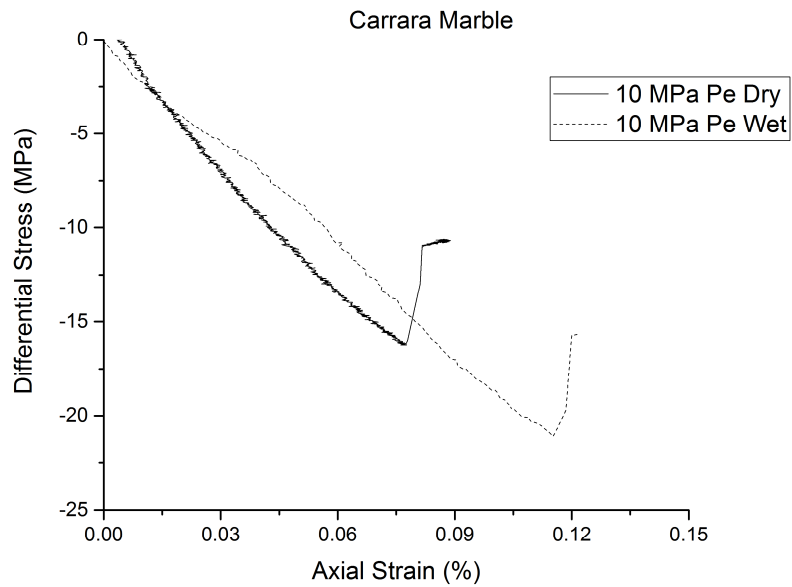


Figure 3. Carrara marble: Axial Strain vs Axial Stress wet and dry at 10 MPa effective confining pressure.

The Indiana Limestone, at 20 MPa effective confining pressure, has a wet and dry strength of ~21 MPa and the dry strength ~14.5 MPa, , at 40 MPa effective confining pressure, has a wet and dry strength of ~40 MPa. The strain at failure is ~0.1% at 20 MPa effective confining pressure and is ~0.17% at 40 MPa effective confining pressure (Figure 4).

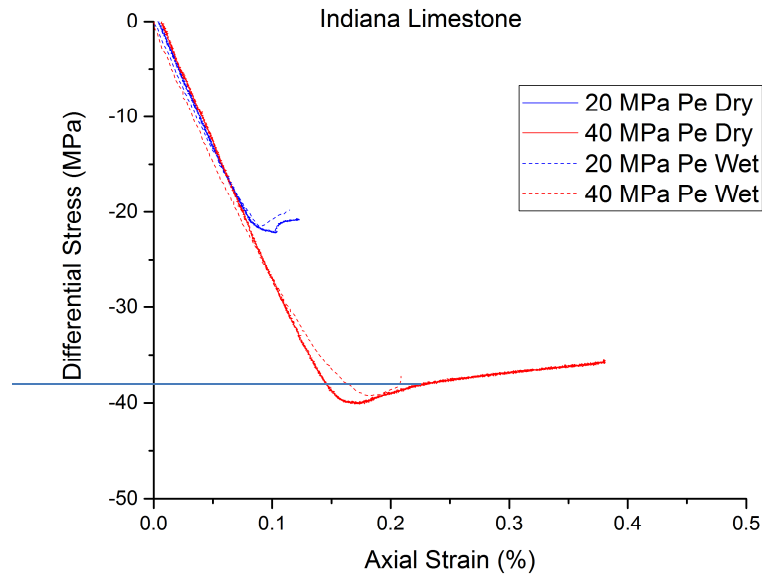


Figure 4. Indiana Limestone: Axial Strain vs Axial Stress wet and dry at 20 MPa and 40 MPa effective confining pressure.

The Kansas Chalk, at 10 MPa effective confining pressure, has a wet and dry strength of 7 MPa and 9.5 MPa, respectively and at 5 MPa effective confining pressure, have a wet and dry strength of 12 MPa and 5.5 MPa, respectively. The strength for the isopropanol test at 5 MPa effective confining pressure is ~5.5 MPa. The dry samples ended in a fracture at 0.2 to 0.3% axial strain, whereas the two water wet tests did not end in fracture; the isopropanol test appeared fully ductile and non-fractured, but was fractured upon removal.

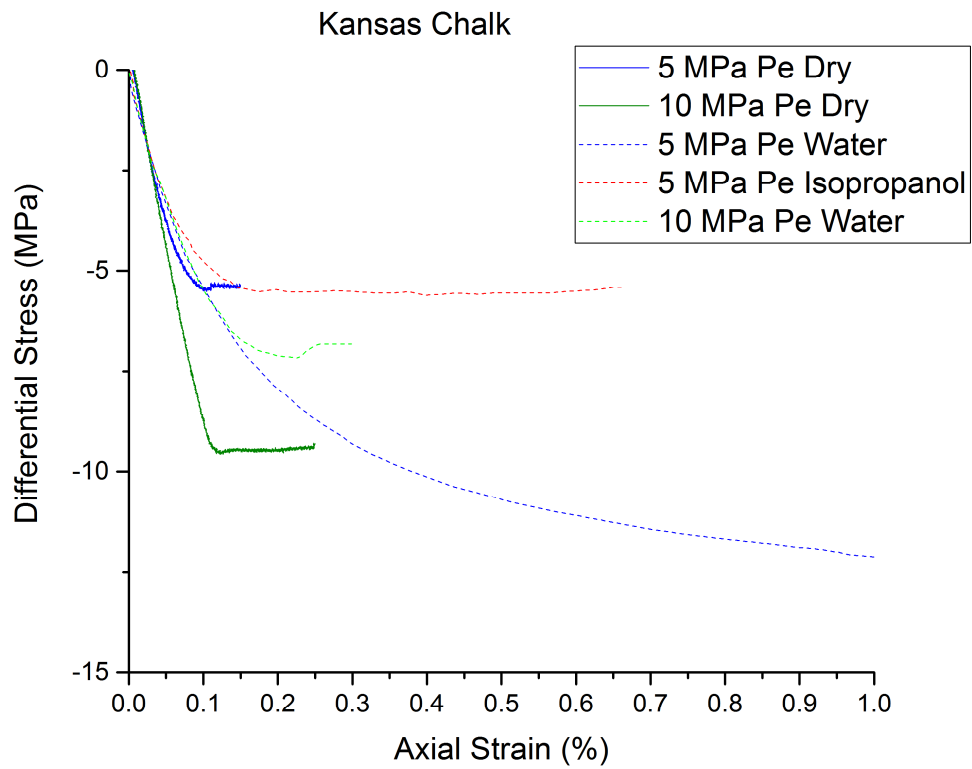


Figure 5. Kansas Chalk: Axial Strain vs Axial Stress wet and dry at 10 MPa and 5 MPa effective confining pressure.

Image Comparison Results

The Berea Sandstone samples, wet and dry, appear quite similar in terms of low (tensile) fracture angle, and fracture smooth surface roughness (Figure 6). The Carrara Marble samples, wet and dry, appear quite similar in terms of low (tensile) fracture angle, and smooth fracture surface roughness (Figure 7). The Indiana Limestone samples, wet and dry, at the two test effective confining pressures appear quite similar in terms of low (tensile) fracture angle, and smooth fracture surface roughness (Figure 8) at 20 MPa effective confining pressure, inclined (transitional) fracture angle, and fracture surface roughness (Figure 9) at 40 MPa effective confining pressure.

The Kansas Chalk samples are markedly different wet and dry. The dry samples have a tensile fracture at low effective confining pressure and an inclined fracture at the higher effective confining pressure. The wet counterparts may not have fractured at all, and show localized necking. The isopropanol test visually may be likened best to the 5 MPa dry test.



Figure 6. Berea sandstone: Dry: top; Wet: bottom at 10 MPa effective confining pressure.

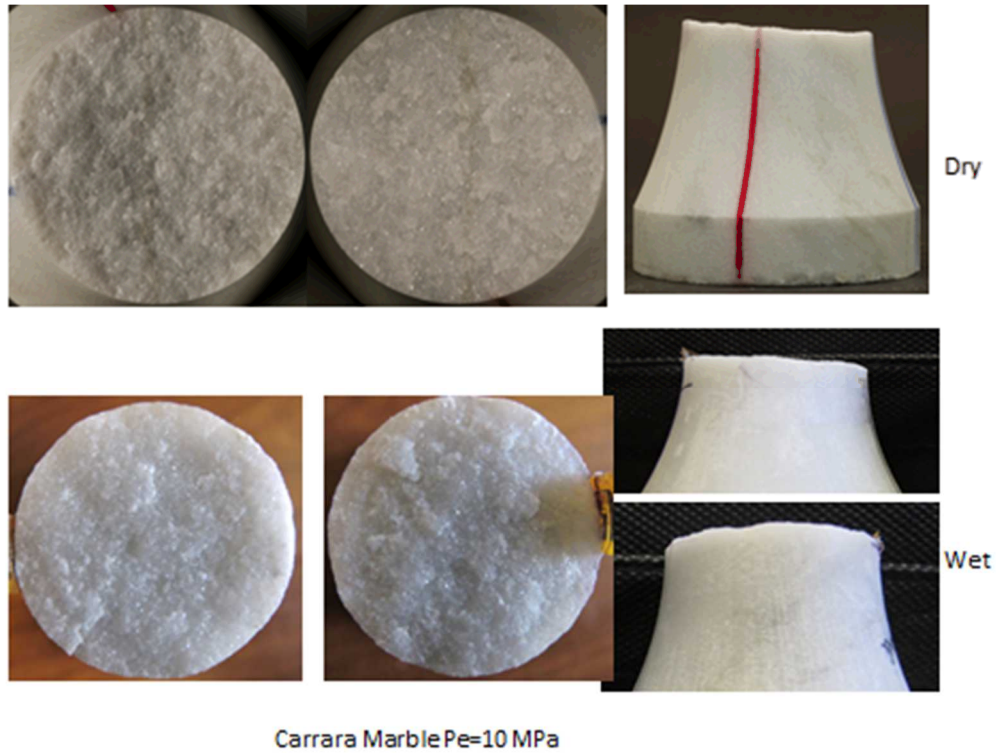


Figure 7. Carrara Marble: Dry: top; Wet: bottom at 10 MPa effective confining pressure.



Figure 8. Indiana Limestone: Dry: top; Wet: bottom at 20 MPa effective confining pressure.



Figure 9. Indiana Limestone: Dry: top; Wet: bottom at 40 MPa effective confining pressure.



Figure 10. Kansa Chalk: Dry: top; Wet: bottom at 5 MPa effective confining pressure.



Figure 11. Kansa Chalk: Dry: top; Wet: bottom at 5 MPa effective confining pressure.

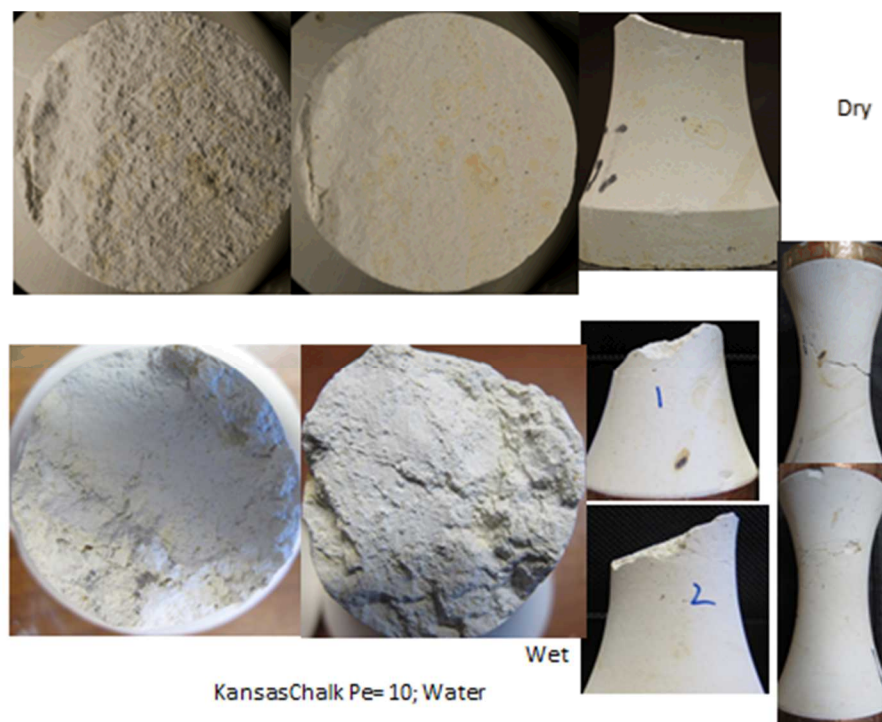


Figure 12. Kansa Chalk: Dry: top; Wet: bottom at 10 MPa effective confining pressure.

DISCUSSION:

The stress strain behavior and observations of deformed wet and dry Berea Sandstone indicate similar material response (strength and ductility) and fracture characteristics; no chemical effect of water is evident at these test conditions, and in this highly porous and permeable rock the effective stress principle appears to work.

The stress strain behavior and observations of deformed wet and dry Carrara Marble indicate the wet rock to be stronger than the dry rock and for the wet rock to experience more strain at failure than the dry rock. Here, in water saturated extension conditions, we have produced experimental evidence of “dilatancy hardening”. The water in the cracks and pores was unable to flow fast enough during the imposed deformation rate to maintain an effective confining pressure as outwardly monitored. Rather, as cracks were forming, the absence of a uniform pore pressure resulted in a strengthening of the rock. This again supports documentation of the effective stress principal but in a negative way.

The stress strain behavior and observations of deformed wet and dry Indiana Limestone indicate very similar material response (strength and ductility) and fracture characteristics; no chemical effect of water is evident at these test conditions, and in this highly porous and permeable rock the effective stress principle is again clearly demonstrated.

The stress strain behavior and observations of deformed wet and dry Kansa Chalk indicate very different material response (strength and ductility) and deformation/fracture characteristics. There is the potential for chemical of water at these test conditions, and in this highly porous and low permeability rock the effective stress principle may come into play. The isopropanol test – being most likened to the dry test in terms of strength, ductility, and fracture characteristics, indicates that the water wet test results may be chemo-water impacted. The few wet tests on this rock beg for more testing of this lithology.

ANTICIPATED IMPACT:

This study is meant to document a select small number of tests upon water saturated counterparts of an extensive dry suite of tests in extension (Choens et al, in prep). In the entire body of work, an experimental suite has been completed using advanced instrumentation and experimental methods wherein a specific sample geometry was used to measure the material behavior of a suite of lithologies in extension. The most recent study includes a set of water saturated experiments. The lithologies chosen investigated the strength of rocks of differing strengths and ductility. The work specifically provides a characterization of rock properties at in situ conditions and demonstrates ways to manipulate material response. The work provides insight to in situ permeability modification through fracture initiation. Finally, this study provides a glimpse of the impact of pore water and pore water pressure upon rock behavior in extension.

CONCLUSIONS:

For three of the rocks types tested in water saturated extension, it was clearly demonstrated that the effective stress principle is valid. Further, no chemo-mechanical effects appear to have expressed themselves for three of the lithologies. Such an effect appears to affect the chalk material response.

REFERENCES:

- Bobich, J. K. (2005), Experimental analysis of the extension to shear fracture transition in Berea sandstone, Texas A&M.
- Choens, R.C., Chester, F.M., Bauer, S.J. An Experimental Investigation into Localization Phenomena in the Tensile to Shear Transition. In Preparation
- Choens, R.C., Chester, F.M., Bauer, S.J. An Experimental Investigation into Hydraulic Fracture Behavior. In Preparation.
- Fredrich, J. T., B. Evans, and T. F. Wong (1989), Micromechanics of the brittle to plastic transition in Carrara marble, *Journal of Geophysical Research-Solid Earth and Planets*, 94(B4), 4129-4145, doi:10.1029/JB094iB04p04129.
- Herrin, E. A. (2008), Experimental study of shear and compaction band formation in Berea sandstone, Texas A&M University, College Station, Texas.
- Hillard, J. E., and L. R. Lawson (2003), *Stereology and Stochastic Geometry*, Kluwer Academic Publishers, Dordrecht, The Netherlands.
- Labuz, J. F., and J. M. Bridell (1993), Reducing frictional constraint in compression testing through lubrication, *International Journal of Rock Mechanics and Mining Sciences & Geomechanics Abstracts*, 30(4), 451-455.
- Menendez, B., W. L. Zhu, and T. F. Wong (1996), Micromechanics of brittle faulting and cataclastic flow in Berea sandstone, *J. Struct. Geol.*, 18(1), 1-16.
- Pieri, M., L. Burlini, K. Kunze, I. Stretton, and D. L. Olgaard (2001), Rheological and microstructural evolution of Carrara marble with high shear strain: results from high temperature torsion experiments, *J. Struct. Geol.*, 23(9), 1393-1413, doi:10.1016/s0191-8141(01)00006-2.
- Ramsey, J. M., and F. M. Chester (2004), Hybrid fracture and the transition from extension fracture to shear fracture, *Nature*, 428(6978), 63-66, doi:10.1038/nature02333.
- Rodriguez, E. (2005), A microstructural study of the extension-to-shear fracture transition in Carrara marble, Texas A&M University.
- Zhang, J. X., T. F. Wong, T. Yanagidani, and D. M. Davis (1990), Pressure-induced microcracking and grain crushing in Berea and Boise sandstones - Acoustic emission and quantitative microscopy measurements, *Mech. Mater.*, 9(1), 1-15.